Letter

Tunable Planar Josephson Junctions Driven by Time-Dependent Spin-Orbit Coupling

David Monroe,[1,*] Mohammad Alidoust,[2,†] and Igor Žutić[1,‡]

[1] *University at Buffalo, State University of New York, Buffalo, New York 14260-1500, USA*

[2] *Department of Physics, Norwegian University of Science and Technology, Trondheim N-7491, Norway*

(Received 18 April 2022; revised 10 July 2022; accepted 2 August 2022; published 15 September 2022; corrected 20 March 2023)

The integration of conventional superconductors with common III–V semiconductors provides a versatile platform to implement tunable Josephson junctions (JJs) and their applications. We propose that with gate-controlled time-dependent spin-orbit coupling, it is possible to strongly modify the current-phase relations and Josephson energy and provide a mechanism to drive the JJ dynamics, even in the absence of any bias current. We show that the transition between stable phases is realized with a simple linear change in the strength of the spin-orbit coupling, while the transition rate can exceed the gate-induced electric field gigahertz changes by an order of magnitude. The resulting interplay between the constant effective magnetic field and changing spin-orbit coupling has direct implications for superconducting spintronics, the control of Majorana bound states, and emerging qubits. We argue that topological superconductivity, sought for fault-tolerant quantum computing, offers simpler applications in superconducting electronics and spintronics.

DOI: 10.1103/PhysRevApplied.18.L031001

In the push to implement beyond-CMOS applications, Josephson junctions (JJs) have found their broad use due to their high-speed switching, low-power dissipation, and intrinsic nonlinearities [1,2]. In addition to the well-established role of JJs as the key elements for superconducting electronics and superconducting qubits [1–6], there is a growing interest in tailoring their spin-dependent properties to enable dissipationless spin currents, cryogenic memory [7–14], and fault-tolerant quantum computing [15–22]. The role of spin-orbit coupling (SOC) has been extensively studied in the normal-state properties and recognized for its importance in spintronics [23–25]. However, the superconducting analogs of the SOC-related effects remain to be understood. They might even be important when their normal-state counterparts are negligibly small [26–32]. Motivated by the recent progress in gate-controlled SOC in planar JJs based on a two-dimensional electron gas (2DEG) [33–35], we reveal how time-dependent SOC tunes many of their key properties and offers an unexplored mechanism to drive JJs.

A common description of a JJ circuit is given by a Josephson element, resistor, and capacitor connected in parallel, using the resistively and capacitively shunted junction (RSCJ) [1] model. The bias current through the junction, i, is the sum of the supercurrent and the quasiparticle current flowing in the resistor and capacitor. The supercurrent is usually assumed as $I(\varphi) = I_c \sin(\varphi + \varphi_0)$, where I_c is the maximum supercurrent, φ is the phase difference between the superconducting regions, and the anomalous phase, $\varphi_0 \neq 0, \pi$, arises from the broken time-reversal and inversion symmetries [37–43].

For a ballistic JJ depicted in Fig. 1(a), the interplay between SOC and the effective Zeeman field, $\mathbf{h}$, yields a more complex current-phase relation (CPR) than $I(\varphi)$ given above, such that for a generalized RSCJ model,

$$d^2\varphi/d\tau^2 + (d\varphi/d\tau)/\sqrt{\beta_c} + I(\varphi, \mu, \mathbf{h}, \alpha)/I_c = i/I_c, \quad (1)$$

where $\tau = \omega_p t$ is a dimensionless time, expressed using the JJ plasma frequency, $\omega_p = \sqrt{2\pi I_c/\Phi_0 C}$, $\Phi_0 = h/2e$ is the magnetic flux quantum, and C is the capacitance. The damping of this nonlinear oscillator is characterized by the Stewart-McCumber parameter, $\beta_c = 2\pi I_c C R^2/\Phi_0$, where R is the resistance [44,45] and $Q = \sqrt{\beta_c}$ is the quality factor. The generalized CPR can be modified by the chemical potential μ, and $\mathbf{h}$, arising from the applied magnetic field or magnetic proximity effect [46]. Since h_z does not induce φ_0 [47,48] and only produces CPR reversals, we focus on $h_z = 0$ [Fig. 1(a)]. The CPR can also be tuned by the Rashba SOC, illustrated in Fig. 1(a), which is parametrized by its strength α, in the Hamiltonian $H_{so} = \alpha(\boldsymbol{\sigma} \times \mathbf{p}) \cdot \hat{\mathbf{z}}$. Here, $\boldsymbol{\sigma}$ is the Pauli matrix vector and

*davidmonroe2016@gmail.com
†phymalidoust@gmail.com
‡zigor@buffalo.edu

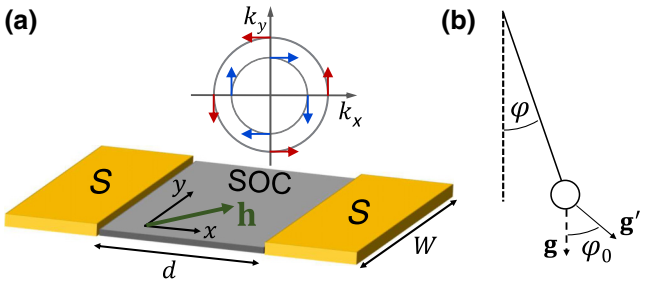

FIG. 1. (a) A schematic of the Josephson junction (JJ). Two s-wave superconductors (S) are separated by the middle region, which hosts the Rashba spin-orbit coupling (SOC), with the depicted **k**-space spin-orbit fields and an effective Zeeman field **h**. (b) A mechanical pendulum model of the JJ. The displacement angle φ is analogous to the superconducting phase difference and **g** is the gravitational acceleration for vanishing SOC and **h**. The pendulum is driven by changing the effective $\mathbf{g}'$, an interplay between **h** and time-dependent SOC. This yields a tunable current-phase relation and an anomalous phase, φ_0, equivalent to the equilibrium of the displaced pendulum.

p is the in-plane momentum, for 2DEG with the inversion symmetry broken along the z direction [49].

While quasistatic gate-tunable changes in SOC and φ_0 have been demonstrated in 2DEG-based JJs [33,34], the implications of dynamically tuned SOC on the CPR remain unexplored. For a conventional CPR without any φ_0, Eq. (1) has a mechanical analog with a driven and damped pendulum, in which φ becomes the displacement angle [44,45]. A JJ driven by i is equivalent to the pendulum displaced by an external torque from its stable equilibrium, determined by the gravitational acceleration **g**, while ω_p determines the oscillation frequency around a stable equilibrium point [1].

Instead of using i, Fig. 1(b) suggests an entirely different way to drive the pendulum: by changing the orientation of the effective $\mathbf{g}'$ and the new equilibrium, resulting from the interplay of the static **h** and time-dependent α. With JJ advances and gate changes exceeding the gigahertz range [3], there is a tantalizing prospect for dynamically controlled CPR by time-dependent SOC. Unlike assuming a specific relation, $I(\varphi) = I_c \sin(\varphi + \varphi_0)$, the CPR can have a more general and anharmonic form that should be obtained microscopically. To this end, a single-particle Hamiltonian, $H(\mathbf{p}) = \mathbf{p}^2/2m^* + \boldsymbol{\sigma} \cdot \mathbf{h} + H_{\rm so}(\mathbf{p})$, where m^* is the effective mass, can be used to solve a BCS model of superconductivity, given by the effective Hamiltonian

$$\mathcal{H}(\mathbf{p}) = \begin{pmatrix} H(\mathbf{p}) - \mu\hat{1} & \hat{\Delta} \\ \hat{\Delta}^\dagger & -H^\dagger(-\mathbf{p}) + \mu\hat{1} \end{pmatrix}, \qquad (2)$$

where $\hat{\Delta}$ is a 2×2 superconducting gap in spin space [47].

After diagonalizing the resulting Bogoliubov–de Gennes equations, $\mathcal{H}\hat{\psi} = E\hat{\psi}$, where $\hat{\psi}$ is the four-component wave function for quasiparticle states with energy E, we match the wave functions and generalized velocities at interfaces ($x = 0, d$), shown in Fig. 1(a). This allows us to obtain the ground-state JJ energy $E_{\rm GS}$, together with the corresponding CPR, using charge conservation and the quantum definition of current [47]. The CPR is related to the JJ energy: $I(\varphi) \propto \partial E_{\rm GS}/\partial\varphi$ [50].

Our numerical findings are illustrated for the JJ depicted in Fig. 1(a). The normal region (N) has a length $d = 0.3\xi_S$ and a width $W = 10d$, such that lengths are normalized by $\xi_S = \hbar/\sqrt{2m^*\Delta}$, where Δ is the superconducting gap in S. The energies are normalized by Δ and the supercurrent $I_0 = 2|e\Delta|/\hbar$, where e is the electron charge and $|e\Delta|/\hbar$ is the maximum supercurrent in a single-channel short S-N-S JJ [50].

To explore the tunability of CPRs and JJ energies with SOC, we focus on the parameters for high-quality epitaxial Al-InAs-based JJs, $\Delta_{\rm Al} = 0.2$ meV, with a g factor of 10 for InAs, while its m^* is 0.03 times the electron mass [33,34]. In these JJs, the gate control of Rashba SOC and thus its magnitude in the range $\alpha \in (0,\ 180$ meVÅ) has been demonstrated [33,34]. In Fig. 2, at $h_x = (2/3)\Delta \approx 450$ mT, we assume a gate control process that primarily changes α, not μ. Experimentally, this could be realized with dual-gate schemes [51] to independently tune the carrier density and the electric field, **E**. However, for a continuous change of α, we are unaware that even in a static case the calculated CPR and $E_{\rm GS}$ are given.

In Fig. 2(a), for $\mu = \Delta$, the anharmonic CPR changes significantly with α. There is a competition between $\sin\varphi$ and the next harmonic, $\sin 2\varphi$, resulting in $I(-\varphi) = -I(\varphi)$. However, there is no spontaneous current, $I(\varphi = 0) \equiv 0$, but only I_c reversal with α. Such a continuous and symmetric 0–π transition is well studied without SOC in S-ferromagnet-S JJs due to the changes in the effective magnetization, temperature, or the thickness of the magnetic

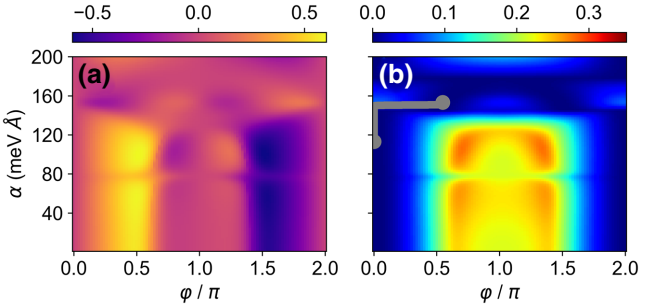

FIG. 2. (a) The evolution of (a) JJ CPR, normalized by $2|e\Delta|/\hbar$, and (b) the JJ energy, normalized by Δ, as a function of the phase φ and the Rashba SOC, α, for chemical potential $\mu = \Delta$ and effective in-plane magnetic field $h_x = (2/3)\Delta$. The gray curve in (b) denotes the JJ transition from $\varphi = 0$ to approximately $\pi/2$ for a linear increase in α from 112 to 152 meVÅ.

region [52–60]. The corresponding JJ energy landscape in Fig. 2(b), shifted such that its overall minimum value is 0, confirms this SOC evolution. By increasing α from 0 to 200 meVÅ, the minimum in $E_{\rm GS}$ changes from $\varphi = 0$ to π and then goes back to 0. A gray trace indicates that by increasing α in a smaller range, the JJ minimum can transition from $\varphi = 0$ to approximately $\pi/2$.

While we use an exact (complete) CPR with its anharmonicities, their prior descriptions have often relied on an approximate simple harmonic expansion ($\sin n\varphi$, $\cos n\varphi$) [61,62]. However, this approach is not very efficient with SOC. Instead, it is better to use a compact form where only a small number of terms gives a more accurate description [47]:

$$I(\varphi,\mu,\mathbf{h},\alpha) \approx \sum_{n=1}^{N}\sum_{\sigma=\pm}\frac{I_n^\sigma \sin(n\varphi+\varphi_{0n}^\sigma)}{\sqrt{1-\tau_n^\sigma \sin^2(n\varphi/2+\varphi_{0n}^\sigma/2)}}, \tag{3}$$

where τ_n^σ is the JJ transparency for spin channel σ and the phase shifts φ_{0n} are additional fitting parameters. This description includes the anomalous Josephson effect $I(\varphi = 0) \neq 0$, revisited in JJ diode effects [63–67]. For a simple picture of a single anomalous phase [47,48],

$$\varphi_0 \propto h_y\alpha^3, \tag{4}$$

therefore vanishing in Fig. 2, where $\mathbf{h} = h_x\hat{x}$.

A quasistatic gate-controlled SOC suggests that more important opportunities are available using fast gate changes, compatible with the advances in JJ circuits [3]. However, the implications of gigahertz changes in SOC and a different mechanism to drive JJ, as sketched in Fig. 1(b), remain unexplored. To obtain the resulting JJ dynamics, we use Eq. (1) with $i \equiv 0$, where the driving arises from $\alpha = \alpha(t)$, viewed as a time-dependent effective $\mathbf{g}'$.

Some guidance as to what to expect for JJ dynamics can be given from the Al-InAs samples, where, in addition to the previous range of α, $I_c \sim 4\ \mu$A, $R \sim 100\ \Omega$, and $C \sim 15$ fF, leading to $\omega_p \sim 900$ GHz and the damping $\beta_c \sim 1$, which is also suitable for the rapid single-flux quantum (RSFQ) applications [1,4]. We keep $h_x = (2/3)\Delta$.

The JJ dynamics are driven by a simple linear variation of $\alpha(t)$ from the gate-controlled **E**, as shown in Fig. 3(a). We first consider, in Fig. 3(b), the reduction of ω_p, from 1000 GHz (similar to Al-InAs JJs [33]) to 10 GHz (much faster than the $\alpha(t)$ variation), at $\beta_c = 1$. The results reveal a strong delay in the onset of the $\varphi = 0$ to approximately $\pi/2$ transition, which is indicated from the static picture in Fig. 2(b). Simultaneously, the time for the $\varphi = 0$ to approximately $\pi/2$ transition is increased by an order of magnitude.

We next examine, in the inset of Fig. 3(b), the influence of reducing β_c from the underdamped and critical ($\beta_c =$ 10 and 1) to the overdamped ($\beta_c = 0.1$) regime, at $\omega_p =$ 1000 GHz. In addition to the phase-oscillation damping, consistent with the pendulum model in Fig. 1(b), we also see a delay in the $\varphi = 0$ to approximately $\pi/2$ transition and its growth, the trends noted from reducing ω_p.

Finally, in Fig. 3(c), the $\varphi = 0$ to approximately $\pi/2$ transition occurs first for the slower $\alpha(t)$ variation but takes approximately the same time as the faster gigahertz $\alpha(t)$ variation. This is encouraging for various applications, since (i) **E** control of SOC allows tailoring of the onset of the transition between different states and (ii) a high-frequency switching between different equilibrium states and driving JJs is not limited by the characteristic times for the **E** variation. The $\alpha(t)$ changes at 0.2 GHz give an order-of-magnitude faster transition between the stable phases.

While the **E** control of α and the evolution of the $E_{\rm GS}$ minima in Fig. 2 largely determine the JJ dynamics in Fig. 3, it helps to identify other opportunities for SOC-driven JJs. In Fig. 4, we consider $\omega_p = 10$ GHz and a triangularlike $\alpha(t)$ at $\mu = 10\Delta$. For an underdamped regime, $\beta_c = 10$, the pendulum analogy from Fig. 1(b) explains the phase evolution of the gray trajectory from Fig. 4(a), also reproduced in Fig. 4(c). By increasing α to the maximum at 192 meVÅ, the pendulum is at an unstable position and will swing toward the $\varphi = 0$ minimum (equivalently shown as $\varphi = 2\pi$), implying that $\mathbf{g}'$ points vertically down. With small damping (gray trajectory), the pendulum passes the equilibrium point even when, with $\alpha < 80$ meVÅ, the equilibrium and the overall minimum shift to $\varphi = \pi$, with

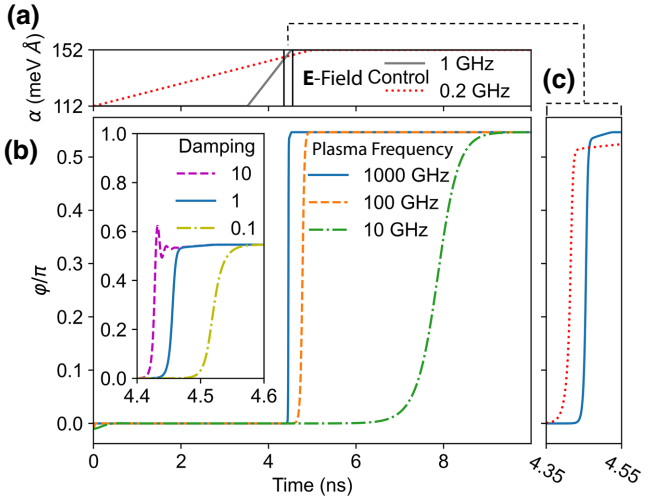

FIG. 3. (a) A time-dependent Rashba SOC, α, controlled by the **E** field, changing at 0.2 GHz and 1 GHz and also used in (b). (b) The time-dependent phase for different plasma frequencies, ω_p, at damping, $\beta_c = 1$, and for different β_c at $\omega_p = 1000$ GHz (inset). (c) A zoomed-in region for the $\varphi = 0$ to approximately $\pi/2$ transition at 0.2 GHz (1 GHz), the dotted line (the solid line), displays changes in α from (a).

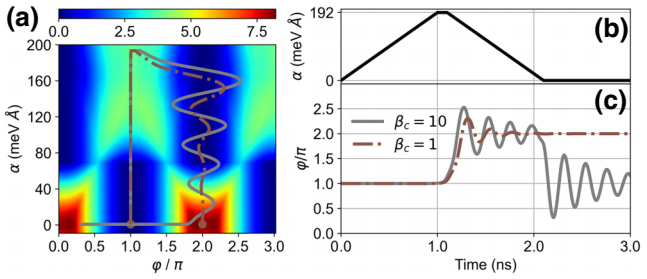

FIG. 4. (a) The JJ energy evolution with φ and α at $\mu = 10\Delta$ and $h_x = (2/3)\Delta$. The gray (brown) curve shows the energy variation for $\beta_c = 10$ ($\beta_c = 1$) starting at $\varphi = \pi$ and $\alpha = 0$, for changing α, as given in (b). (c) The corresponding time-dependent φ confirms the decay to different final phase states.

$\mathbf{g}'$ vertically up. Eventually, with damping, it reaches the $\varphi = \pi$ minimum.

For critical damping, with the same starting point [see also Fig. 4(c)], the brown trajectory reveals a very different evolution with α. Instead, at the overall E_{GS} minimum $\varphi = \pi$, for $\alpha = 0$, the phase is locked at the local minimum $\varphi = 0$. With a stronger damping, the φ oscillations are insufficient to overcome the SOC-dependent barrier, which, for $\alpha = 0$, separates the local minimum at $\varphi = \pi$ from the global one at $\varphi = 2\pi$. The tunability of the SOC-controlled energy landscape alone does not fully determine the generalized CPRs. The influence of the JJ circuit parameters can enable different φ transitions.

In the above discussion, the tunability of CPRs and E_{GS} does not exploit the anomalous Josephson effect [37–40,70], which can be understood in analogy to $\mathbf{g}'$ pointing sideways and, therefore, breaking the symmetry from Figs. 2–4 and $I(-\varphi) \neq -I(\varphi)$. This situation can be simply realized by rotating $\mathbf{h}$ along the y axis, while we retain

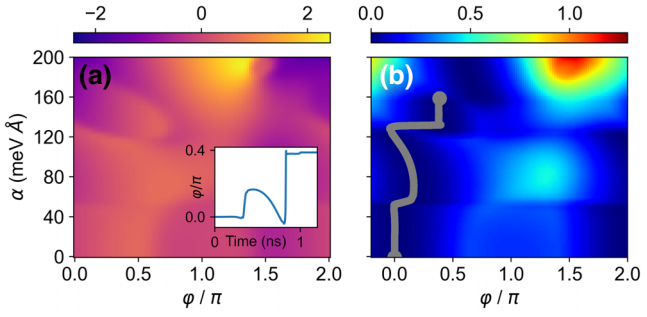

FIG. 5. The evolution of (a) JJ CPR and (b) the JJ energy with φ and α, for $\mu = \Delta$ and $h_y = (2/3)\Delta$, rotated by $\pi/2$ from Fig. 2. An anharmonic CPR breaks the $I(-\varphi) = -I(\varphi)$ symmetry in (a) and the corresponding anomalous phase, φ_0, increases with α in (b). The inset in (a) shows $\varphi(t)$ for $\omega_p = 1000$ GHz, $\beta_c = 1$, with a linearly increasing α from 0 to 160 meVÅover 1 ns, which is then held at a maximum, with its JJ energy path in (b).

all the other parameters from Fig. 2(a). The resulting CPR in Fig. 5(a) confirms that the JJ supercurrent is driven not only by φ but also by φ_0, which is responsible for the stated symmetry breaking and, equivalently, the tilted $\mathbf{g}'$. As for SOC cubic in $\mathbf{k}$ [47], there is a strong anharmonic behavior and the expected diode effect, where the sign and magnitude of the supercurrent depend on the polarity of the applied bias [34].

The implications of the combined broken time-reversal and inversion symmetries, responsible for the anomalous Josephson effect, are further illustrated in Fig. 5(b), which shows the SOC-tunable E_{GS}, single valued for the gray path and leading to the time-dependent diode effect. This behavior is qualitatively different from the doubly degenerate φ_0 state in Fig. 2(b), which results from the second-harmonic generation in the CPR.

Even with a moderate $h_y \approx 450$ mT for InAs-based JJs, with increasing $\alpha(t)$ we see an evolution of the single global minimum and thus the changes in the corresponding values of φ_0 from $\varphi = 0$ to approximately $3\pi/4$, in good agreement with the measured values [33]. This suggests that at a larger $\mathbf{h}$, for example, in In(As,Sb) with a much larger g factor [35], it may be possible to fully control the tilt angle of $\mathbf{g}'$ and simply swap between 0 and π states in JJs, further controlling how the JJ dynamics are driven.

The same geometry in Al-InAs JJs at a larger h_y has been experimentally shown to also support topological superconductivity [34]. This is important for several reasons, beyond hosting Majorana bound states [16]. The resulting topological superconductivity is associated with equal-spin p-wave superconductivity, which could offer gate-controlled dissipationless spin currents, a key element for superconducting spintronics [7,8]. Such spin-triplet supercurrents could be extended over a long range [71] and could overcome the usual competition between superconductivity and ferromagnetism. A transition to topological superconductivity is accompanied by an extra phase jump of approximately π [72,73]. Such a π jump in Al-InAs JJs has been observed at $h_y \approx 600$ mT [34], an effective field about 25 times smaller than expected for the 0–π transition:

$$B_{0\text{-}\pi} = (\pi/2)\hbar v_{\mathrm{F}}/(g\mu_{\mathrm{B}}d), \tag{5}$$

for a spin-polarized system in the absence of SOC [74], where v_{F} is the Fermi velocity, μ_{B} the Bohr magneton, and d is the JJ length. Therefore, SOC plays a crucial role in understanding various transitions and, at larger h_y, the range of an effective φ_0 could exceed 2π [34] and support 2π pendulum rotation from Fig. 1(b), as used in RSFQ logic and memory [1,4]. Therefore, in addition to the prospect of fault-tolerant quantum computing, the search for topological superconductivity also offers a promising platform for superconducting electronics and spintronics.

Without previous studies on SOC-driven JJ dynamics, we focus on a simple model and do not consider time-dependent magnetic fields [75] or noise [76]. A more general description could simultaneously include the role of changing μ and other SOC forms, linear and cubic in $\mathbf{k}$, shown to give different routes to topological superconductivity and control of Majorana states [47,77–79]. However, we expect that our focus only on linearized Rashba SOC, easily tunable by the $\mathbf{E}$ field [33,34], already clarifies its important role in JJ dynamics. With changing SOC, there are further opportunities for gate-controlled Majorana states and the probing of their non-Abelian statistics [80,81] or an added tunability in the implementation of superconducting qubits [3,82,83]. This would extend the previously studied qubit tunability by voltage or flux [3,84] as well as the use of π-phase states for an improved qubit operation [85,86].

Acknowledgments.—We thank Javad Shabani and Tong Zhou for valuable discussions. This work is supported by the National Science Foundation (NSF) Electrical, Communications and Cyber Systems (ECCS) Grant No. 2130845, the U.S. Office of Naval Research (ONR) through Grants No. N000141712793 and MURI No. N000142212764 (D. M. and I. Ž.), and the University at Buffalo Center for Computational Research.

[1] F. Tafuri, ed. *Fundamentals and Frontiers of the Josephson Effect* (Springer Nature, Cham, 2019).
[2] M. Siegel and M. Hidaka, in *Nanoelectronics and Information Technology 3rd Ed.*, edited by R. Wasner (Wiley-VCH, Weinheim, Germany 2012), p. 421.
[3] P. Krantz, M. Kjaergaard, F. Yan, *et al.*, Appl. Phys. Rev. **6**, 021318 (2019).
[4] K. K. Likharev and V. K. Semenov, IEEE Trans. Appl. Supercond. **1**, 3 (1991).
[5] D. S. Holmes, A. L. Ripple, and M. A. Manheimer, IEEE Trans. Appl. Supercond. **23**, 1701610 (2013).
[6] F. Giazotto, J. T. Peltonen, M. Meschke, *et al.*, Nat. Phys. **6**, 254 (2010).
[7] M. Eschrig, Rep. Prog. Phys. **78**, 104501 (2015).
[8] J. Linder and J. W. A. Robinson, Nat. Phys. **11**, 307 (2015).
[9] T. S. Khaire, M. A. Khasawneh, W. P. Pratt, *et al.*, Phys. Rev. Lett. **104**, 137002 (2010).
[10] N. Banerjee, J. W. A. Robinson, and M. G. Blamire, Nat. Commun. **5**, 4771 (2014).
[11] E. C. Gingrich, B. M. Niedzielski, J. A. Glick, *et al.*, Nat. Phys. **12**, 564 (2016).
[12] N. O. Birge and M. Houzet, IEEE Magn. Lett. **9**, 4509605 (2019).
[13] A. A. Mazanik, I. R. Rahmonov, A. E. Botha, and Yu. M. Shukrinov, Phys. Rev. Appl. **14**, 014003 (2020).
[14] W. Han, S. Maekawa, and X.-C. Xie, Nat. Mater. **19**, 139 (2020).
[15] L. Fu and C. L. Kane, Phys. Rev. Lett. **100**, 096407 (2008).
[16] D. Aasen, M. Hell, R. V. Mishmash, *et al.*, Phys. Rev. X **6**, 031016 (2016).
[17] K. Laubscher and J. Klinovaja, J. Appl. Phys. **130**, 081101 (2021).
[18] U. Güngördü and Alexey A. Kovalev, Majorana bound states with chiral magnetic textures, preprint.
[19] L. P. Rokhinson, X. Liu, and J. K. Furdyna, Nat. Phys. **8**, 795 (2012).
[20] A. Fornieri, A. M. Whiticar, F. Setiawan, *et al.*, Nature **569**, 89 (2019).
[21] H. Ren, F. Pientka, S. Hart, *et al.*, Nature **569**, 93 (2019).
[22] M. M. Desjardins, L. C. Contamin, M. R. Delbecq, *et al.*, Nat. Mater. **18**, 1060 (2019).
[23] I. Žutić, J. Fabian, and S. Das Sarma, Rev. Mod. Phys. **76**, 323 (2004).
[24] J. Fabian, A. Matos-Abiague, C. Ertler, *et al.*, Acta Phys. Slov. **57**, 565 (2007).
[25] D. Bercioux and P. Lucignano, Rep. Prog. Phys. **78**, 106001 (2015).
[26] I. Högl, A. Matos-Abiague, I. Žutić, *et al.*, Phys. Rev. Lett. **115**, 116601 (2015).
[27] A. Costa, P. Högl, and J. Fabian, Phys. Rev. B **95**, 024514 (2017).
[28] P. Lv, Y.-F. Zhou, N.-X. Yang, *et al.*, Phys. Rev. B **97**, 144501 (2018).
[29] I. Martínez, P. Högl, C. González-Ruano, *et al.*, Phys. Rev. Appl. **13**, 014030 (2020).
[30] T. Vezin, C. Shen, J. E. Han, *et al.*, Phys. Rev. B **101**, 014515 (2020).
[31] C. González-Ruano, L. G. Johnsen, D. Caso, *et al.*, Phys. Rev. B **102**, 020405(R) (2020).
[32] R. Cai, Y. Yao, P. Lv, *et al.*, Nat. Commun. **12**, 6725 (2021).
[33] W. Mayer, M. C. Dartiailh, J. Yuan, *et al.*, Nat. Commun. **11**, 21 (2020).
[34] M. Dartiailh, W. Mayer, J. Yuan, *et al.*, Phys. Rev. Lett. **126**, 036802 (2021).
[35] An even larger Rashba SOC is possible in other JJs [36].
[36] W. Mayer, W. F. Schiela, J. Yuan, *et al.*, ACS Appl. Electron. Mater. **2**, 2351 (2020).
[37] A. A. Reynoso, G. Usaj, C. A. Balseiro, *et al.*, Phys. Rev. Lett. **101**, 107001 (2008).
[38] A. Buzdin, Phys. Rev. Lett. **101**, 107005 (2008).
[39] F. Konschelle and A. Buzdin, Phys. Rev. Lett. **102**, 017001 (2009).
[40] H. Sickinger, A. Lipman, M. Weides, *et al.*, Phys. Rev. Lett. **109**, 107002 (2012).
[41] E. Strambini, A. Iorio, O. Durante, *et al.*, Nat. Nanotechnol. **15**, 656 (2020).
[42] Yu. M. Shukrinov, Phys. Usp. **65**, 317 (2022).
[43] I. I. Soloviev, V. I. Ruzhickiy, S. V. Bakurskiy, N. V. Klenov, M. Yu. Kupriyanov, A. A. Golubov, O. V. Skryabina, and V. S. Stolyarov, Phys. Rev. Appl. **16**, 014052 (2021).
[44] W. C. Stewart, Appl. Phys. Lett. **12**, 277 (1968).
[45] D. E. McCumber, J. Appl. Phys. **39**, 3113 (1968).
[46] I. Žutić, A. Matos-Abiague, B. Scharf, *et al.*, Mater. Today **22**, 85 (2019).
[47] M. Alidoust, C. Shen, and I. Žutić, Phys. Rev. B **103**, L060503 (2021).

[48] M. Alidoust, Phys. Rev. B **101**, 155123 (2020).
[49] Y. A. Bychkov and E. I. Rashba, Pis'ma Zh. Eksp. Teor. Fiz. **39**, 66 (1984), JETP Lett. **39**, 78 (1984).
[50] A. Zagoskin, *Quantum Theory of Many-Body Systems* (Springer, New York, 2014), 2nd ed.
[51] D. Van Tuan, B. Scharf, Z. Wang, *et al.*, Phys. Rev. B **99**, 085301 (2019).
[52] T. Kontos, M. Aprili, J. Lesueur, *et al.*, Phys. Rev. Lett. **89**, 137007 (2002).
[53] V. V. Ryazanov, V. A. Oboznov, A. Yu. Rusanov, *et al.*, Phys. Rev. Lett. **86**, 2427 (2001).
[54] F. S. Bergeret, A. F. Volkov, and K. B. Efetov, Rev. Mod. Phys. **77**, 1321 (2005).
[55] M. Eschrig, J. Kopu, J. C. Cuevas, *et al.*, Phys. Rev. Lett. **90**, 137003 (2003).
[56] K. Halterman, O. T. Valls, and C.-T. Wu, Phys. Rev. B **92**, 174516 (2015).
[57] C.-T. Wu and K. Halterman, Phys. Rev. B **98**, 054518 (2018).
[58] O. T. Valls, *Superconductor/Ferromagnet Nanostructures* (World Scientific, Hackensack, NJ, 2022).
[59] T. Yamashita, A. Kawakami, and H. Terai, Phys. Rev. Appl. **8**, 054028 (2017).
[60] T. Yamashita, S. Takahashi, and S. Maekawa, Phys. Rev. B **73**, 144517 (2006).
[61] A. A. Golubov, M. Yu. Kupriyanov, and E. Il'ichev, Rev. Mod. Phys. **76**, 411 (2004).
[62] S. Kashiwaya and Y. Tanaka, Rep. Prog. Phys. **63**, 1641 (2000).
[63] F. Ando, Y. Miyasaka, T. Li, *et al.*, Nature **574**, 373 (2020).
[64] Y. Y. Lyu, Ji Jiang, Y.-L. Wang, *et al.*, Nat. Commun. **12**, 2703 (2021).
[65] C. Baumgartner, L. Fuchs, A. Costa, *et al.*, Nat. Nanotechnol. **17**, 39 (2021).
[66] K. Halterman, M. Alidoust, R. Smith, *et al.*, Phys. Rev. B **105**, 104508 (2022).
[67] An early proposal for such a diode effect did not require SOC [68]. A superconducting diode effect is also possible with a single *S* region [69].
[68] J. Hu, C. Wu, and X. Dai, Phys. Rev. Lett. **99**, 067004 (2007).
[69] N. F. Q. Yuan and L. Fu, Proc. Natl. Acad. Sci. USA **119**, e2119548119 (2022).
[70] Y. Xu, P.-H. Fu, L. Chen, *et al.*, Phys. Rev. B **105**, 075409 (2022).
[71] J. R. Eskilt, M. Amundsen, N. Banerjee, *et al.*, Phys. Rev. B **100**, 224519 (2019).
[72] M. Hell, M. Leijnse, and K. Flensberg, Phys. Rev. Lett. **118**, 107701 (2017).
[73] F. Pientka, A. Keselman, E. Berg, *et al.*, Phys. Rev. X **7**, 021032 (2017).
[74] T. Yokoyama, M. Eto, and Y. V. Nazarov, Phys. Rev. B **89**, 195407 (2014).
[75] M. Nashaat, A. E. Botha, and Yu. M. Shukrinov, Phys. Rev. B **97**, 224514 (2018).
[76] D. Massarotti, N. Banerjee, R. Caruso, *et al.*, Phys. Rev. B **98**, 144516 (2018).
[77] B. Pekerten, J. D. Pakizer, B. Hawn, *et al.*, Phys. Rev. B **105**, 054504 (2022).
[78] J. D. Pakizer, B. Scharf, and A. Matos-Abiague, Phys. Rev. Res. **3**, 013198 (2021).
[79] B. Scharf, F. Pientka, H. Ren, *et al.*, Phys. Rev. B **99**, 214503 (2019).
[80] T. Zhou, M. C. Dartiailh, K. Sardashti, *et al.*, Nat. Comun. **13**, 1738 (2022).
[81] P. P. Paudel, T. Cole, B. D. Woods, *et al.*, Phys. Rev. B **104**, 155428 (2021).
[82] A. Bargerbos, M. Pita-Vidal, R. Žitko, *et al.*, Singlet-doublet transitions of a quantum dot Josephson junction detected in a transmon circuit, arXiv:2202.12754.
[83] M. Hays, V. Fatemi, D. Bouman, *et al.*, Science **373**, 6553 (2021).
[84] L. Casparis, M. R. Connolly, M. Kjaergaard, *et al.*, Nat. Nanotechnol. **13**, 915 (2018).
[85] T. Yamashita, K. Tanikawa, S. Takahashi, *et al.*, Phys. Rev. Lett. **95**, 097001 (2005).
[86] S. Kawabata, S. Kashiwaya, Y. Asano, *et al.*, Phys. Rev. B **74**, 180502(R) (2006).

Correction: The references were styled inconsistently during the proof production process and have been rectified. A proof request to change *L* to *d* in the second sentence of the second paragraph after Eq. (2), in Eq. (5), and in the text following Eq. (5) was not done and has now been implemented. The hyperlink was not active in Ref. [36] and has been fixed.